Supporting Information

Single-precursor-derived carbon and nitrogen co-doped CuO nanozymes for colorimetric detection of tetracycline

Yu Liu,[a] Jingjing Fang,[a] Liangxiao Jiang,[a] Hengchao Yang,[a] Cheng Yao*[a] and Chan Song*[a]

[a.] *School of Chemistry and Molecular Engineering, Nanjing Tech University, Nanjing 211816, China.*

Email: yaocheng@njtech.edu.cn; songchan@njtech.edu.cn

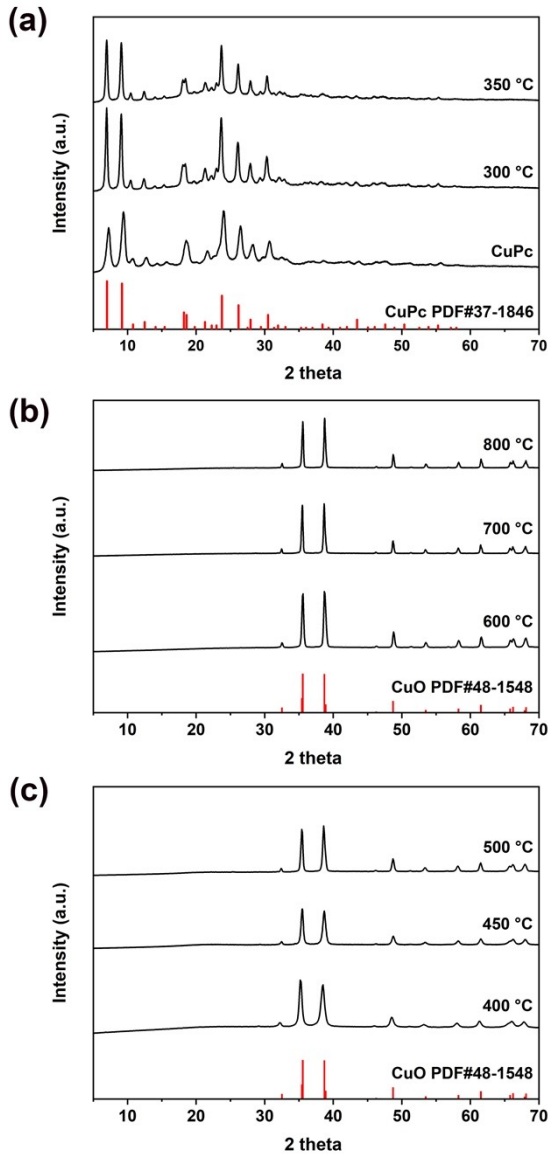

Figure S1. XRD patterns of CuPc and materials obtained by pyrolyzing CuPc(II) at the reaction temperatures ranged from 300 °C to 800 °C.

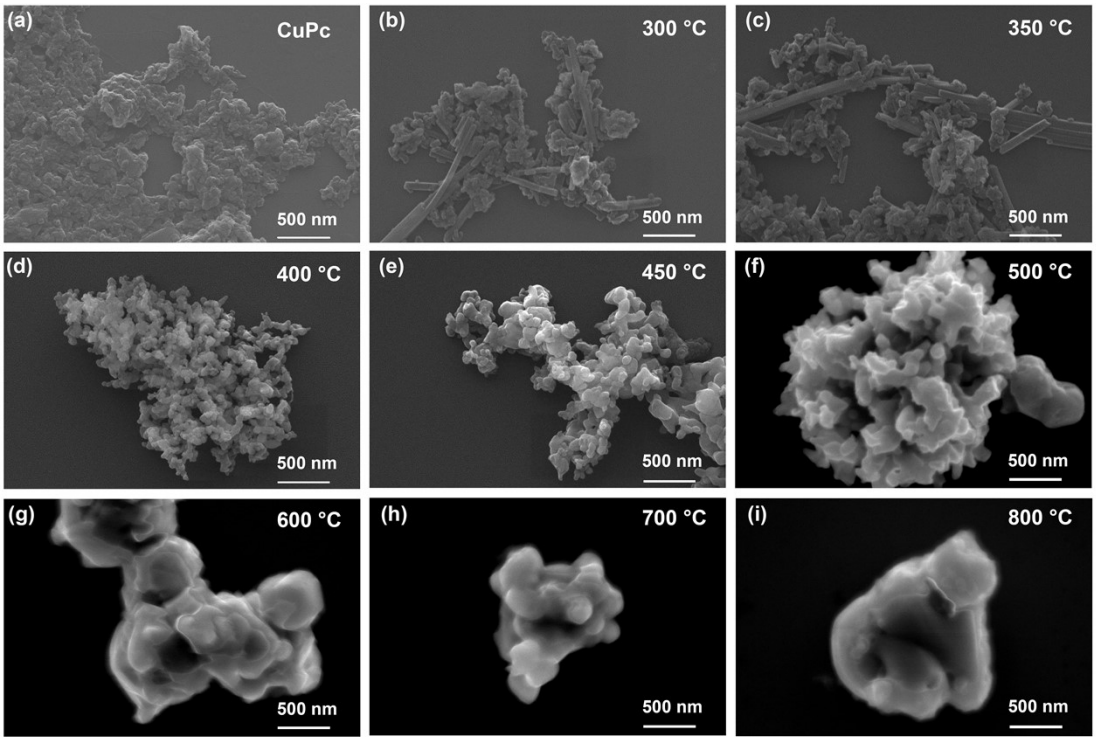

Figure S2. SEM images of CuPc and materials obtained by pyrolyzing CuPc(II) at the reaction temperatures ranged from 300 °C to 800 °C.

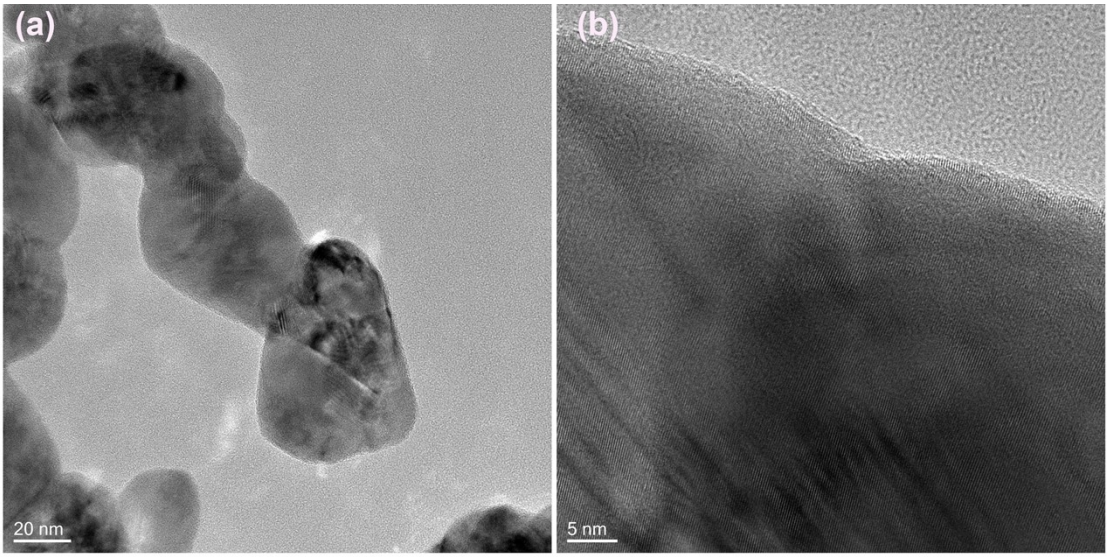

Figure S3. Typical TEM image (a) and HRTEM image (b) of C-N/CuO-400.

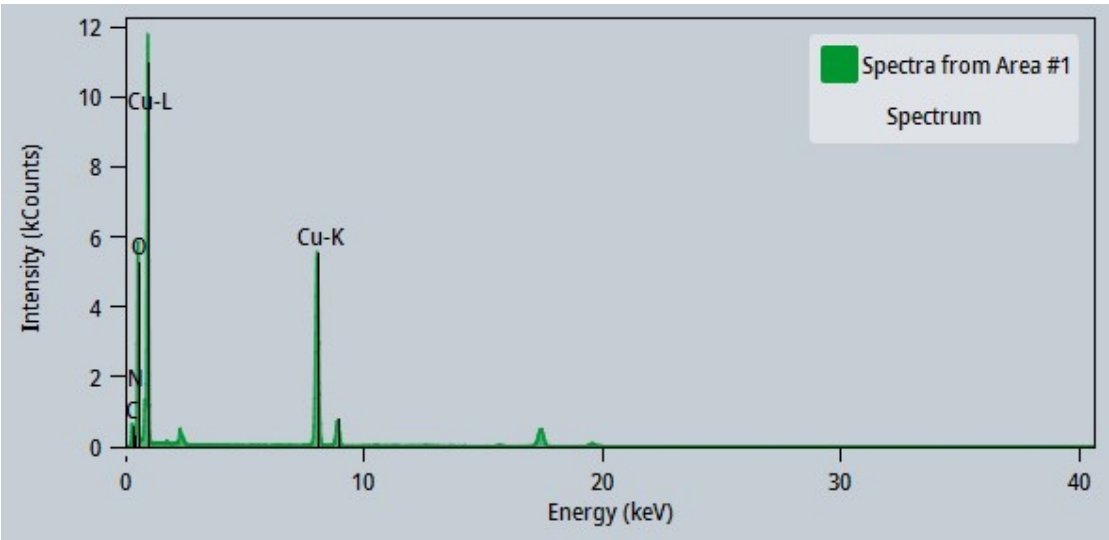

Figure S4. EDX spectrum of C-N/CuO-400.

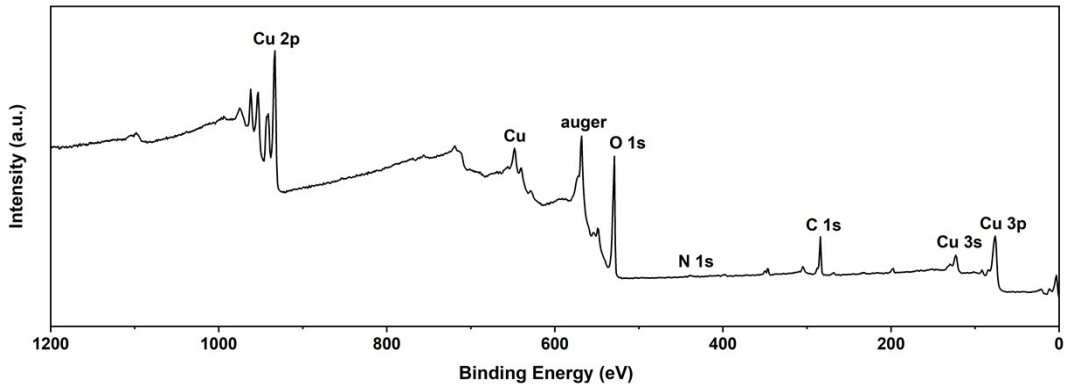

Figure S5. XPS spectrum of C-N/CuO-400.

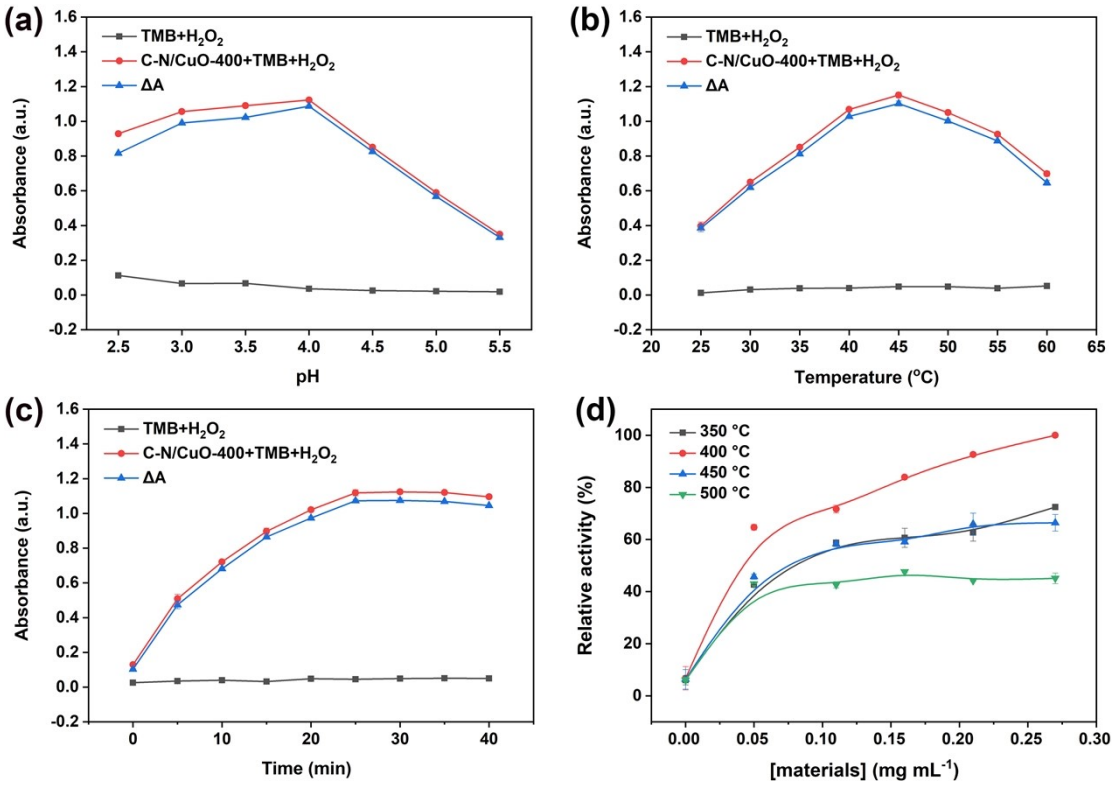

Figure S6. The absorbance intensity at 652 nm of TMB and H_2O_2 with and without C-N/CuO-400 at different pH (a), temperature (b), and incubation time (c). ΔA = A-A_0, A and A_0 was the absorbance intensity of TMB and H_2O_2 with and without C-N/CuO-400, respectively. (d) The absorbance intensity at 652 nm of TMB and H_2O_2 with different amounts of materials calcined at different temperatures.

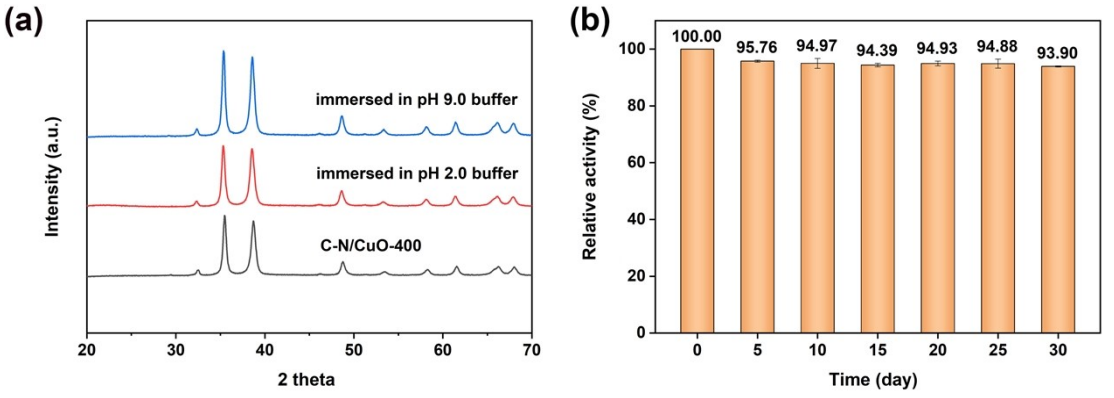

Figure S7. (a) XRD patterns of C-N/CuO-400 and C-N/CuO-400 immersed in different pH buffer for 30 minutes. (b) Stability of the catalytic property provided by C-N/CuO-400.

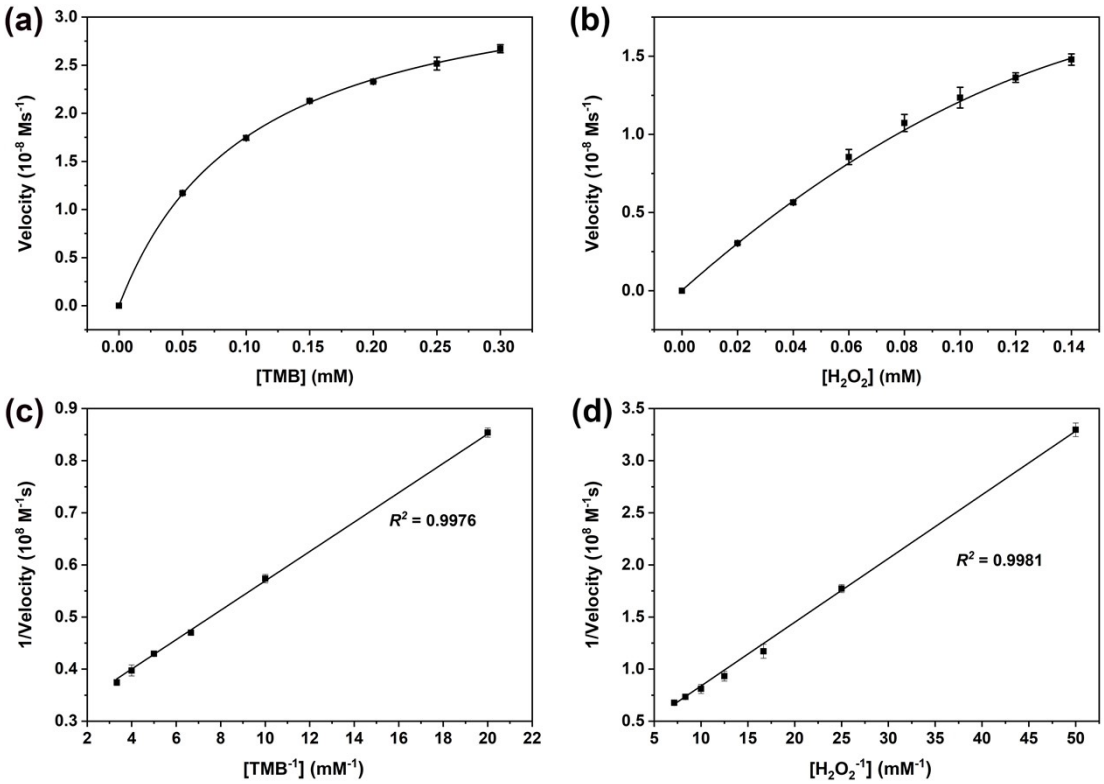

Figure S8. Steady-state kinetic analyses of C-N/CuO-400 using the Michaelis-Menten model (a and b) and the Lineweaver-Burk double inverse model (c and d).

Table S1. The kinetic parameters of oxidation reaction catalyzed by horseradish peroxidase (HRP) and some enzyme-like nanomaterials.

Catalysts	TMB		H_2O_2		Reference
	K_m (mM)	V_{max} (10^{-8} M s^{-1})	K_m (mM)	V_{max} (10^{-8} M s^{-1})	
HRP	0.43	10.00	3.70	8.71	[1]
CuO/Pt NFs	0.33	27.86	0.75	12.88	[2]
Cu-Cu_2O/PtPd	0.34	12.78	0.28	2.41	[3]
PAN-CuO	0.09	4.68	0.58	20.14	[4]
CuO_x	0.46	14.56	1.84	9.57	[5]
Cu_2O/Pt cubes	0.29	2.72	5.82	2.46	[6]
C-N/CuO-400	**0.098**	**3.48**	**0.27**	**4.42**	**This work**

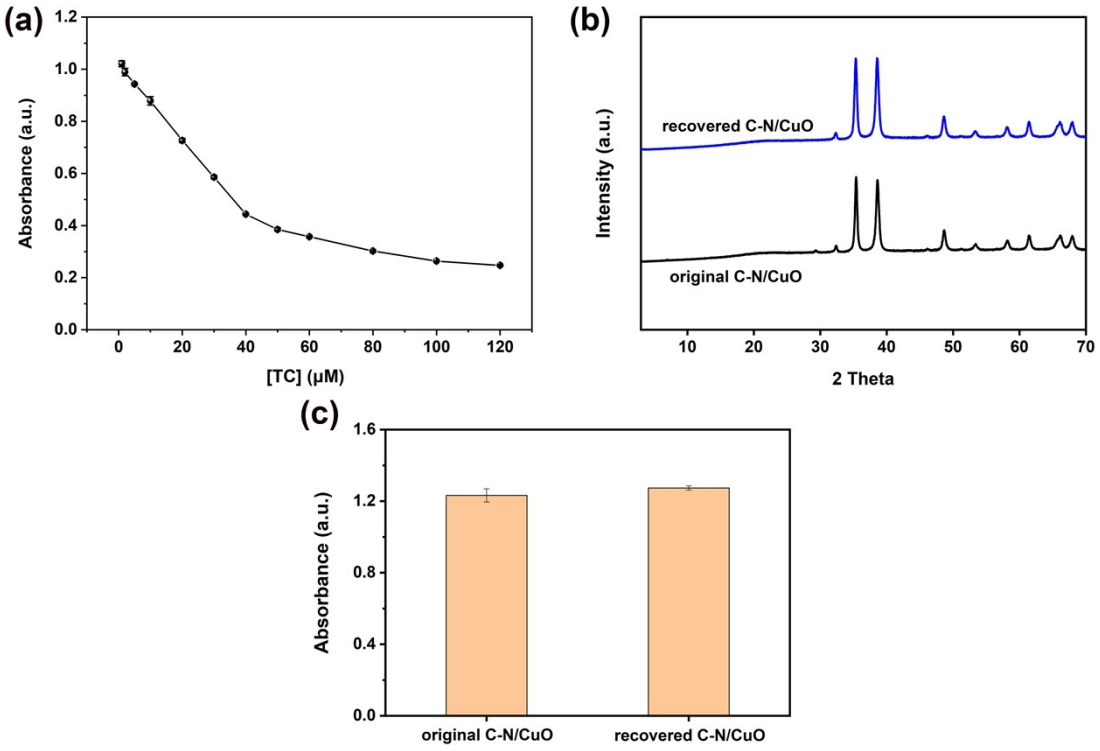

Figure S9. (a) The absorption intensity at 652 nm of C-N/CuO-400-based catalytic system with different concentration of TC. XRD patterns (b) and catalytic activity tests (c) of the original and recovered C-N/CuO-400 after the TC detection process.

Table S2. Linear ranges and detection limits of different nanomaterial-based methods for TC detection.

Materials	Methods	Detection limit (μM)	Linear range (μM)	Reference
D-Trp-OMe@AuNCs	Colorimetry	0.20	1.5-30.0	[7]
PEI-SQDs	Fluorometric	0.15	0.20-100.0	[8]
LLCDs	Fluorometric	0.42	0-27.27	[9]
N-CQDs	Fluorometric	0.34	0-100.0	[10]
MIP-AA/CQDs	Fluorometric	0.17	1.0-60.0	[11]
C-N/CuO-400	**Colorimetry**	**0.15**	**1.0-40.0**	**This work**

Table S3. Recovery of spiked TC from actual samples.

Samples	Spiked (μM)	Recovered (μM)			Recovery (%)	RSD (%)
	20	20.36	20.22	20.36	101.56	0.40
Lake water	30	29.70	29.84	30.11	99.61	0.71
	40	38.76	39.38	40.29	98.69	1.95
Yangtze	20	19.80	19.03	19.52	97.26	1.99
River	30	31.02	29.98	30.25	101.39	1.78
water	40	39.52	40.15	40.08	99.79	0.86
	20	19.03	20.29	20.57	99.82	4.09
Honey	30	29.42	30.67	30.81	101.00	2.53
	40	38.97	40.08	39.87	99.10	1.50

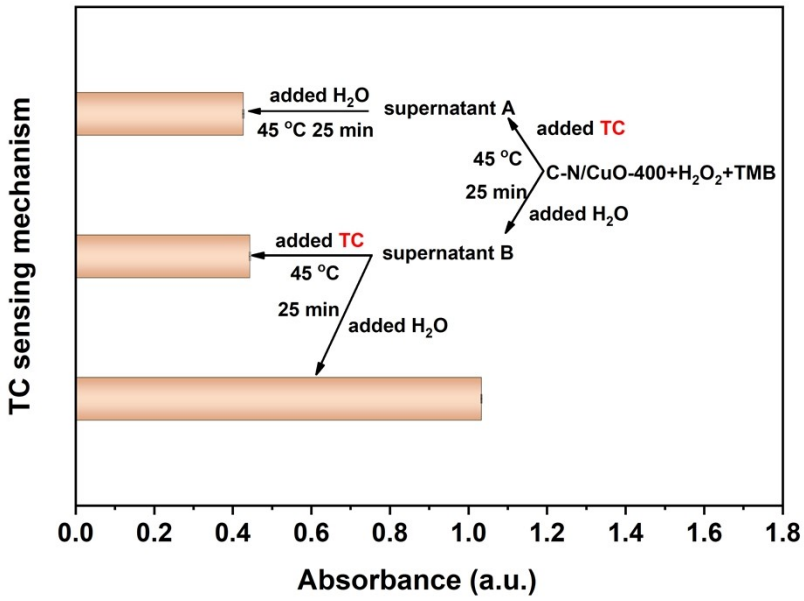

Figure S10. The investigation of TC sensing mechanism by using C-N/CuO-400 as the sensing platform. After the mixtures of C-N/CuO-400, TMB, and H_2O_2 with and without TC, were incubated at 45 ℃ for 25 min, the resulting solutions were followed by centrifugation, achieving the supernatant A and B. Inset illustrates schematic diagrams of different reaction processes. [TC] = 40 μM, [C-N/CuO-400] = 0.16 mg/mL.

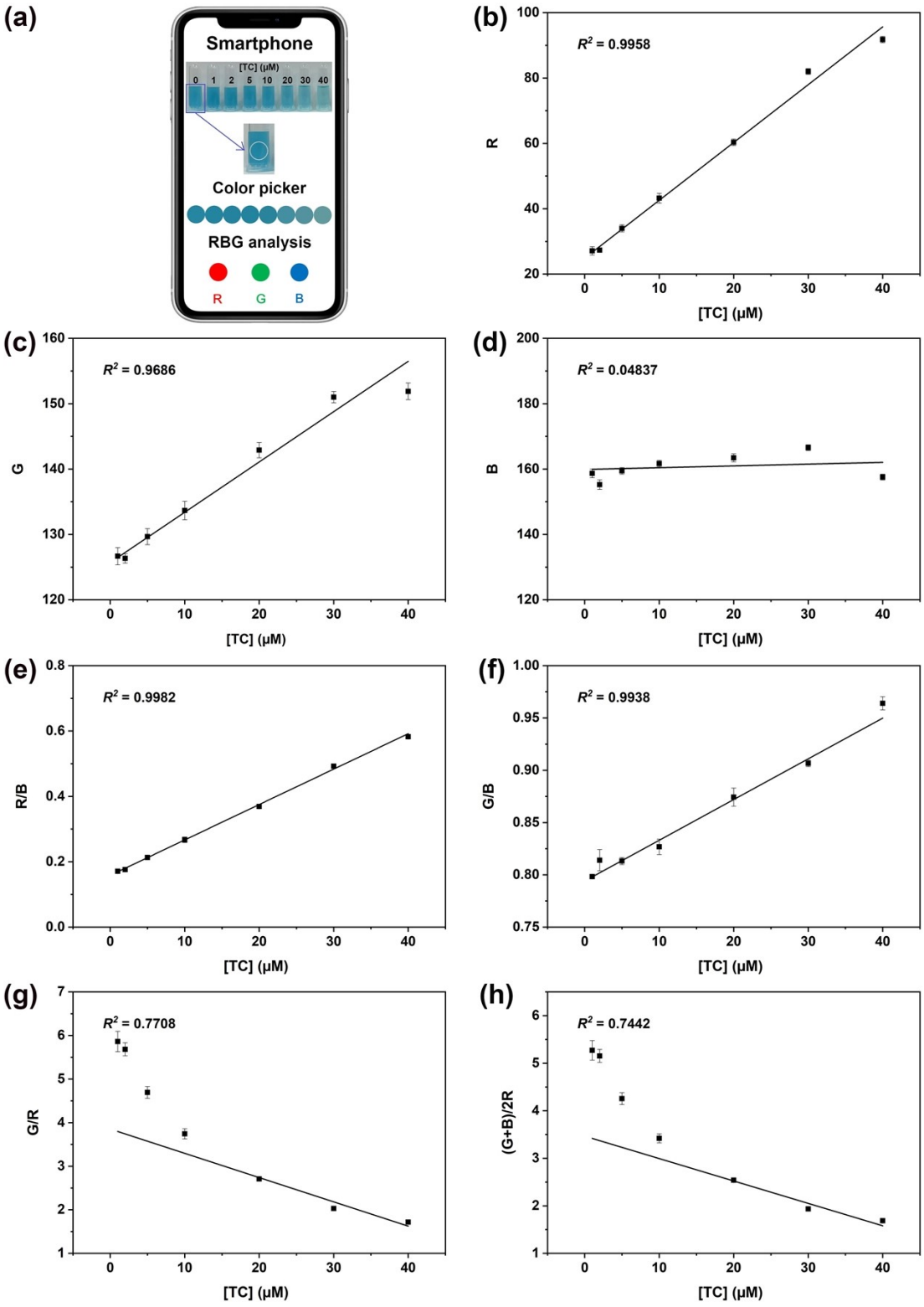

Figure S11. (a) RGB reading diagram of a smart phone. (b-h) Linear relationship between RGB values (or their ratios) and TC concentration in the range of 1-40 μM. TC concentration was 1, 2, 5, 10, 20, 30 and 40 μM, respectively.

Figure S12. The photographs of the TMB-H_2O_2 system catalyzed by C-N/CuO-400 captured using an iPhone 16 Pro Max (n = 6).

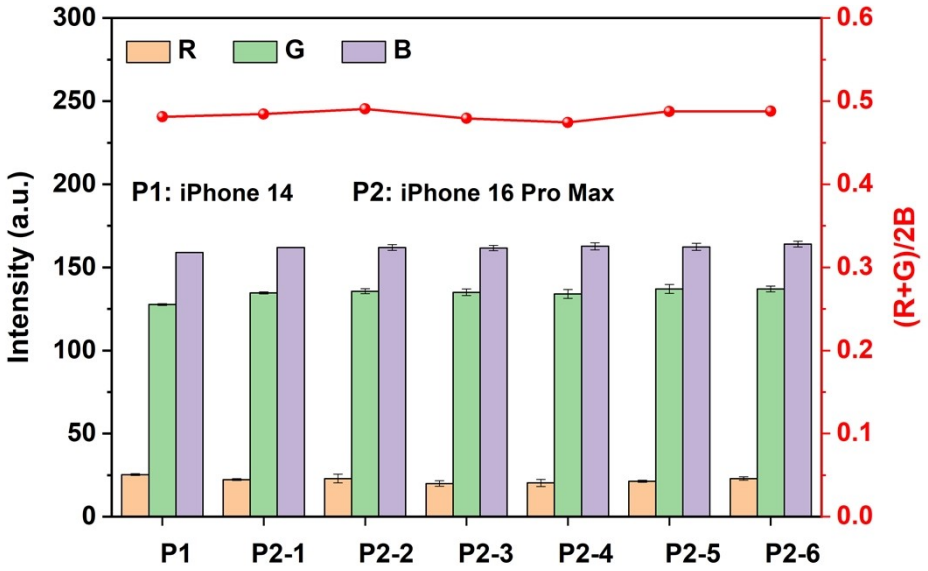

Figure S13. RGB values obtained from photographs of the TMB-H_2O_2 system catalyzed by C-N/CuO-400 captured using iPhone 14 (P1) and iPhone 16 Pro Max (n = 6, P2-1 to P2-6), along with the corresponding calculated (R+G)/2B ratios.

Reference

[1] Gao, L.; Zhuang, J.; Nie, L.; Zhang, J.; Zhang, Y.; Gu, N.; Wang, T.; Feng, J.; Yang, D.; Perrett, S.; et al. Intrinsic peroxidase-like activity of ferromagnetic nanoparticles. Nat. Nanotechnol. 2007, 2, 577-583.

[2] Lian, Q.; Liu, H.; Zheng, X.; Li, X.; Zhang, F.; Gao, J. Enhanced peroxidase-like activity of CuO/Pt nanoflowers for colorimetric and ultrasensitive Hg^{2+} detection in water sample. Appl. Surf. Sci. 2019, 483, 551-561.

[3] Zhao, H.; Li, K.; Zou, Y.; Wang, Y.; Zhong, Z.; Xi, Y.; Xiao, X. Enhanced peroxidase-like activity of Cu-Cu_2O composite film through PtPd immobilization for colorimetric glucose detection. Talanta 2024, 273, 125964.

[4] Zheng, X.; Lian, Q.; Zhou, L.; Jiang, Y.; Gao, J. Peroxidase mimicking of binary polyacrylonitrile-CuO nanoflowers and the application in colorimetric detection of H_2O_2 and ascorbic acid. ACS Sustainable Chem. Eng. 2021, 9, 7030-7043.

[5] Zhang, X.; Xue, C.; Cao, H.; Wu, Y.; Yang, B.; Zhou, T.; Zhai, W.; Deng, J. Ultra-small CuOx/GDYO nanozyme with boosting peroxidase-like activity via electrochemical strategy: Toward applicable colorimetric detection of organophosphate pesticides. Talanta 2024, 279, 126639.

[6] Sun, G.; Zhang, Y.; Qian, D.; Xu, Q.; Li, J.; Li, H. Morphology-controlled peroxidase-like cuprous oxide-platinum cubes for dual-mode sensing of mercury ions. Sens. Actuators B: Chem 2024, 410, 135709.

[7] Song, Y.; Qiao, J.; Liu, W.; Qi, L. Enhancement of gold nanoclusters-based peroxidase nanozymes for detection of tetracycline. Microchem. J. 2020, 157, 104871.

[8] Chang, Y.; He, R.; Wei, Y.; Wang, L. Polyethyleneimine-sulfur quantum dot composites for dual-channel detection of tetracycline by colorimetric and fluorescence sensing. ACS Appl. Nano Mater 2023, 6, 7414-7421.

[9] Venugopalan, P.; Vidya, N. Microwave-assisted green synthesis of carbon dots derived from wild lemon (Citrus pennivesiculata) leaves as a fluorescent probe for tetracycline sensing in water. Spectrochim. Acta Part A: Mol. Biomol. Spectrosc. 2023, 286, 122024.

[10] Wang, C.; Sun, Q.; Yang, M.; Liu, E.; Xue, W.; Fan, J. Preparation of highly luminescent nitrogen-doped carbon quantum dots and their detection of tetracycline antibiotics. Colloids Surf. A: Physicochem. Eng. Asp. 2022, 653, 129982.

[11] Wei, X.; Lv, L.; Zhang, Z.; Guan, W. Preparation of molecularly imprinted fluorescence sensor based on carbon quantum dots via precipitation polymerization for fluorescence detection of tetracycline. J. Appl. Polym. Sci. 2020, 137, e49126.